

# Use of quantum-chemical descriptors to analyse reaction rate constants between organic chemicals and superoxide/hydroperoxyl ( $O_2^{\bullet-}/HO_2^{\bullet}$ )

**Journal Article****Author(s):**

Nolte, Tom M.; Peijnenburg, Willie J.G.M.

**Publication date:**

2018

**Permanent link:**

<https://doi.org/https://doi.org/10.3929/ethz-b-000313483>

**Rights / license:**

[Creative Commons Attribution-NonCommercial-NoDerivatives 4.0 International](#)

**Originally published in:**

Free Radical Research 52(10), <https://doi.org/10.1080/10715762.2018.1529867>



# Use of quantum-chemical descriptors to analyse reaction rate constants between organic chemicals and superoxide/hydroperoxyl ( $O_2^{\bullet-}/HO_2^{\bullet}$ )

Tom M. Nolte & Willie J. G. M. Peijnenburg

To cite this article: Tom M. Nolte & Willie J. G. M. Peijnenburg (2018) Use of quantum-chemical descriptors to analyse reaction rate constants between organic chemicals and superoxide/hydroperoxyl ( $O_2^{\bullet-}/HO_2^{\bullet}$ ), Free Radical Research, 52:10, 1118-1131, DOI: [10.1080/10715762.2018.1529867](https://doi.org/10.1080/10715762.2018.1529867)

To link to this article: <https://doi.org/10.1080/10715762.2018.1529867>



© 2018 The Author(s). Published by Informa UK Limited, trading as Taylor & Francis Group.



Accepted author version posted online: 01 Oct 2018.  
Published online: 13 Nov 2018.



Submit your article to this journal [↗](#)



Article views: 87



View Crossmark data [↗](#)

## Use of quantum-chemical descriptors to analyse reaction rate constants between organic chemicals and superoxide/hydroperoxyl ( $O_2^{\bullet-}/HO_2^{\bullet}$ )

Tom M. Nolte<sup>a,b</sup> and Willie J. G. M. Peijnenburg<sup>c,d</sup>

<sup>a</sup>Department of Environmental Science, Institute for Water and Wetland Research, Radboud University Nijmegen, Nijmegen, the Netherlands; <sup>b</sup>Laboratory of Inorganic Chemistry, Eidgenössische Technische Hochschule (ETH) Zurich, Zurich, Switzerland; <sup>c</sup>National Institute of Public Health and the Environment, Bilthoven, The Netherlands; <sup>d</sup>Institute of Environmental Sciences (CML), Leiden University, Leiden, The Netherlands

### ABSTRACT

The reaction between superoxide ( $O_2^{\bullet-}$ ) and organic chemicals is of interest in many scientific disciplines including biology and synthetic chemistry, as well as for the evaluation of chemical fate in the environment. Due to limited data and lack of congeneric modelling, the involvement of superoxide in many complex processes cannot be adequately evaluated. In this study, we developed new quantitative structure–property relationship (QSPR) models for the prediction of the aqueous-phase rate constant for the reaction between superoxide and a wide variety of organic chemicals reacting via one-electron oxidation, reduction and hydrogen-transfer. It is shown that the relative importance of these pathways is related to frontier molecular orbital (FMO) interaction and to pH. The class-specific QSPRs developed have good statistics ( $0.84 \leq R^2 \leq 0.92$ ). For non-congeneric chemicals it is demonstrated that the reactivity toward superoxide can be described by applying explicit descriptions for competition kinetics and speciation. Therefore, the relationships developed in this study are useful as a starting point to evaluate more complex molecules having, for example, multiple reactive functional groups, labile H bonds, or delocalised cationic charges. However, additional kinetic data and more rigorous computation are needed to evaluate such molecules.

### ARTICLE HISTORY

Received 9 August 2018  
Revised 12 September 2018  
Accepted 25 September 2018



### KEYWORDS


Superoxide; hydroperoxyl; radicals; antioxidants; reaction rate constant; quantitative structure–property relationship; organic chemicals; frontier molecular orbital; kinetics

### Introduction

Molecular oxygen ( $O_2$ ) is involved in many (bio)chemical reactions and can be both beneficial and harmful in nature. Reactions between ground-state  $O_2$  (triplet-state diradical) and singlet-state molecules are spin-forbidden. However, the addition of a second electron fills one of its two degenerate orbitals, yielding a reduced species with one unpaired electron and a net negative charge. The transfer of an electron to  $O_2$  to yield superoxide,  $O_2^{\bullet-}$  (spin-allowed), results in a more reactive species which can participate in both one- and two-electron reactions [1]. Due to its reactivity, superoxide has found use in organic synthesis. Superoxide is versatile; it can function either as an oxidant or reductant depending on the oxidation–reduction potential of the reacting molecule, as an oxygen nucleophile or as a Brønsted base [2,3]. For example, it can be used for substitution and hydrolysis reactions, that is, with alkyl

halides, tosylates and esters [2]. Superoxide is a potential “green” reagent to replace invasive, hazardous, toxicologically and environmentally demanding reagents [3]. For example, Jiang et al. used potassium superoxide ( $KO_2$ ) as an alternative oxidant in a Winterfeldt reaction instead of  $O_2/KOt-Bu$  [4].  $O_2^{\bullet-}$  can convert amines to carbonyl compounds via N-chloramines [5] and to carbamates using tetraethylammonium superoxide and carbon dioxide [6].  $O_2^{\bullet-}$  can also be used to activate reagents such as arenesulfonylperoxy- or arenesulfinylperoxy radicals which can regioselectively epoxidize olefins, desulphurise thiocarbonyls to carbonyls, cleave C=N bonds to C=O, and convert of benzylic methylenes to ketones [7]. Despite the increasing use of  $O_2^{\bullet-}$  in synthesis, reactions are often carried out in “classic” organic solvents such as benzene, chloroform, toluene and DMF. More friendly solvents are bio-based, such as esters, alcohols, terpenes and DMSO [2]. An aqueous

**CONTACT** Tom M. Nolte  [tom.m.nolte@gmail.com](mailto:tom.m.nolte@gmail.com)  Department of Environmental Science, Institute for Water and Wetland Research, Radboud University Nijmegen, Nijmegen, the Netherlands

 Supplemental data for this article can be accessed [here](#).

© 2018 The Author(s). Published by Informa UK Limited, trading as Taylor & Francis Group.

This is an Open Access article distributed under the terms of the Creative Commons Attribution-NonCommercial-NoDerivatives License (<http://creativecommons.org/licenses/by-nc-nd/4.0/>), which permits non-commercial re-use, distribution, and reproduction in any medium, provided the original work is properly cited, and is not altered, transformed, or built upon in any way.

solvent has often been regarded as the apex of green chemistry [8], but its applicability depends very much on the nature of the reagents and the desired reaction. Thus, in order to aid further “greening” of synthetic chemistry, more information is needed on the relative reactivity of  $O_2^{\bullet-}$  toward organic chemicals in aqueous (and bio-based) solvent.

Apart from its use in synthesis, superoxide is biologically relevant [9].  $O_2^{\bullet-}$  can be generated from “leakage” of electrons along the cellular electron transport chain or from quinines, metal complexes, aromatic nitro/amino compounds, or conjugated imines during redox cycling. Since reactions between singlet-state and triplet-state molecules are spin-forbidden, enzymes have to provide mechanisms to adjust the spin value of  $O_2$  (i.e. via reduction to superoxide) or of its substrates. The reductant can be a metal complex or an organic molecule with an accessible radical form [1]. It has been shown that  $O_2^{\bullet-}$  is involved in P450 oxidation in the human liver [10], and is produced intracellularly by flavoenzymes such as xanthine oxidase, lipogenase, cyclooxygenase and the NADPH-dependent oxidase of phagocytic cells.  $O_2^{\bullet-}$  is also generated extracellularly by reduction via cell surface enzymes, or via the release of labile redox-active compounds in the extracellular milieu. In water,  $O_2^{\bullet-}$  has a typical half-life of tens of seconds to hours indicating that  $O_2^{\bullet-}$  can influence local redox chemistry on a scale which is biologically significant. In a typical “healthy” cell, the steady-state intracellular  $O_2^{\bullet-}$  concentration is approximately 100 pM ( $10^{-10}$  M) [11]. Therefore,  $O_2^{\bullet-}$  may react with biomolecules via a chain reaction of free-radical formation. Oxidative stress arises when the cellular production of reactive oxygen species (such as  $O_2^{\bullet-}$ ) overrides the natural anti-oxidant (radical-scavenging) capacity and is an important mechanism that contributes to carcinogenesis in humans [12]. To combat such effects, the human body produces natural anti-oxidants such as superoxide dismutase (SOD) of which the metal-containing active site can alternately react both as a reductant and as an oxidant with  $O_2^{\bullet-}$ . Additionally, anti-oxidants can be taken in via food or supplements.

$O_2^{\bullet-}$  is also ubiquitously present in surface waters [3]. Photolysis of dissolved organic matter (DOM) is a major source of  $O_2^{\bullet-}$ , but microbial activity and photolysis of trace metal complexes may contribute as well.  $O_2^{\bullet-}$  can accumulate in natural water bodies to typical concentrations of  $10^{-11}$  to  $10^{-9}$  M, depending on location and depth. In the upper water column, which receives more sunlight and is biologically more active, the concentration may range from  $10^{-9}$  to  $10^{-7}$  M, as was determined from formation rate experiments [13–16]. These

concentrations are sufficiently high to ensure that  $O_2^{\bullet-}$  can react at environmentally relevant rates and suggest that  $O_2^{\bullet-}$  may be important in the photochemical degradation of various anthropogenic or naturally occurring chemicals [17]. Lastly,  $O_2^{\bullet-}$  has also been detected during advanced (Fenton-type) wastewater treatment in which it contributed to the degradation of chemicals such as atrazine (herbicide) and rhodamine B (dye) [3].

Given the wide involvement of  $O_2^{\bullet-}$  in chemical, biological and environmental processes, knowledge on its relative reactivity toward organic chemicals is crucial. Lots of data is already available for  $O_2^{\bullet-}$  and reactive oxygen species (ROS) in general. In the light of “intelligent” experimentation and cost-effectiveness of (environmental) risk assessment, such data should be used to assess new (untested) chemicals as well. To this end, various quantitative structure–property relationship (QSPR) models have been developed capable of predicting the reactivity of  $O_2^{\bullet-}$  toward “new”, untested compounds [18,19]. Many have investigated the antioxidative capacities of food constituents and supplements such as flavonoids and polyphenols [20,21]. However, most data (and models) have been expressed using qualitative (*in vitro*) assays and chemical descriptors such as lipophilicity and water solubility/hydration energy, that is, bioavailability [22], instead of kinetic parameters more directly describing the chemical reaction. Moreover, many such QSPRs describe general antioxidant activity (e.g. in terms of ROS inhibition), which obscures the proportion of the anti-oxidant activity exerted by  $O_2^{\bullet-}$  specifically [19,23,24].

Different chemical descriptors have been used to explain the reactivity toward  $O_2^{\bullet-}$ . For example, the number of OH groups, bond dissociation energy (BDE), energy of the lowest unoccupied molecular orbital (LUMO), and half peak oxidation potential have been used to describe the antioxidant activity for a range of structurally similar compounds [18,24] reacting via H-abstraction and addition [25]. However, the reaction rate with  $O_2^{\bullet-}$  may also depend on the protonation state of the chemical (which can be affected the medium pH) as was shown for other oxidants, for example, the hydroxyl radical [26,27], manganese(IV) complexes [28] and thiazine dyes [29]. The pH-dependence may be especially relevant to  $O_2^{\bullet-}$  reactions because the superoxide molecule itself is also susceptible to (de)protonation [30]. Many existing QSPRs for “anti-oxidant activity” have limited applicability, being developed for similar (congeneric) chemicals, for example, chalcones [19], flavonoids [18], coumarins [20], arylamines derivatives [31]) only. Evaluation of kinetic data becomes more complicated when different

chemicals, reacting through different mechanisms, are considered together. Chemicals can have complicated structures, characterised by the simultaneous presence of different functional groups and flexible substructures. Hence, more complex QSPRs use descriptors characterising H-bond donor capacity and ortho/para/meta substitution [24]), 3D distribution of electronegative atoms and electrostatic environment [18,31], delocalisation and superdelocalizability. Despite recent progress, the relative importance of structural characteristics and pH/pKa on the reaction rate is still not well understood. Consequently, there are few QSPR models that can predict  $O_2^{\bullet-}$  reactivity across different series of chemicals. Despite the absence of such QSPRs, we hypothesised that it is possible to establish a “global” model using generic QC descriptors, as long as the influence of pH/pKa on reactivity is included explicitly.

In order to evaluate the involvement of superoxide in complex (bio)chemical processes, we aimed to develop a generic QSPR model for the prediction of aqueous-phase reaction rate constants that is applicable across various chemical families. To this end, we reviewed the available kinetic data for superoxide and information on reaction pathways from the literature. Acknowledging the importance of the reaction pathway and charges, we computed quantum-chemical and electro-topological descriptors for specific speciation states and evaluate their relevance to kinetic parameters both empirically and mechanistically.

## Methods

### Data selection

Data for the bimolecular reaction rate constant ( $k_r O_2^{\bullet-}$  and  $k_r HO_2^{\bullet}$ ) was gathered from publications using *Web of Science* and *Google Scholar* search engines (before December 2017). Notable sources were the review by Bielski et al. (1985) [30] and the NDRL/NIST Solution Kinetics Database [32] in which data were categorised based on endpoint, method, similarity of values, etc., allowing comparison and quality selection. The energy and electronic structure of an organic molecule can be significantly altered by pH, as was previously shown to affect kinetic parameters for related oxidants [33]. Hence, for QSPR development (or at least as a starting point therefore), pH should be reported in the experiments. Free radical compounds were excluded due to their relatively high, often diffusion-limited, reactivity (thereby focussing on longer-lived chemicals) and to standardise the calculation of molecular descriptors. The final dataset contained approximately 200 heterogeneous organic chemicals with aqueous-phase rate constants

(Supporting Information Table S1), determined via various methods, mostly using laser flash photolysis and pulse radiolysis (X,  $\gamma$  and e-) techniques [34].

### Descriptor calculation

Since the dataset included ionisable chemicals,  $pK_a$ ,  $pK_b$  and dominant speciation states at experimental pH were taken from literature or (depending on availability) predicted using Chemaxon [35] ( $R^2 = 0.778$ ,  $N = 653$  [36] and  $R^2 = 0.76$ ,  $N = 261$  [37]). This resulted in neutral, anionic, cationic, zwitterionic and multivalent chemical structures. Speciation-specific structures (either protonated or deprotonated depending on experimental pH) were pre-optimised in the gas phase using OpenBabel, version 2.3.0 using the mmff94 force field [38]. Structures were further optimised and quantum chemical (QC) molecular descriptors (MD), for example,  $E_{HOMO}$  (energy of the highest occupied molecular orbital),  $E_{LUMO}$  (energy of the lowest unoccupied molecular orbital), polarizability and dipole moment were calculated semi-empirically (PM7 [39]) using MOPAC (2016) [40] and the COSMO (conductor-like Screening Model) approximation for water (NSPA = 92) [41] implementing the correct net charge on the chemical (Supporting Information Figures S2 and S3), analogous to a previous study [33]. Additional MD were calculated using Chemopy [42] after geometry optimisation with which we attempted to develop a multiple linear regression (MLR) model, but this did not yield satisfactory results (see Supporting Information Figure S4).

### Model building

In water,  $O_2^{\bullet-}$  is in a pH dependent equilibrium with its conjugate acid  $HO_2^{\bullet}$ . However, the  $pK_a$  of  $HO_2^{\bullet}$  is 4.88 [43] which implies that at neutral pH all but 0.3% of superoxide is present as the anion (negatively charged), Equation (1):



Depending on the pH and the chemical evaluated,  $O_2^{\bullet-}/HO_2^{\bullet}$  can react either via oxidation or reduction (Table 1). Although highly variable, the average experimental pH for all the data was approximately 7 (Supporting Information Table S1) which implies that superoxide is most often present in its anionic form ( $O_2^{\bullet-}$ ), increasing the likelihood of a reductive pathway. Preliminary analysis showed that most of the variance (50%) in the data was explained by  $E_{LUMO}$ , with (poly)-phenols and aromatic cations being notable outliers (Supporting Information Figure S1(B)).

**Table 1.** Properties of reactive oxygen species.

ROS property	O <sub>2</sub> <sup>•-</sup>	HO <sub>2</sub> <sup>•</sup>	OH <sup>•</sup> (at pH 7)	<sup>1</sup> O <sub>2</sub> (at pH 7)
$E^{\circ}_{ox/red}$ (V) <sup>a,b,c</sup>	-0.18 <sup>d</sup>	+0.79 <sup>e</sup> +1.46 <sup>f</sup>	+1.902 <sup>g</sup> +2.730 <sup>h</sup>	+0.81 <sup>i</sup>
$E_{SOMO}$ (eV) <sup>j</sup>	-3.8	-5.7	-8.0	-
$\Delta H_f^{\circ}$ (kJ mol <sup>-1</sup> ) <sup>a</sup>	80	138	-7	94.3
[I] <sub>ss</sub> in surface water (M)	10 <sup>-9</sup> – 10 <sup>-7</sup>	10 <sup>-11</sup> – 10 <sup>-9k</sup>	10 <sup>-19</sup> – 10 <sup>-17</sup>	10 <sup>-14</sup> – 10 <sup>-13</sup>
$k_r$ for phenol (M <sup>-1</sup> s <sup>-1</sup> )	5.8 × 10 <sup>21</sup>	2.7 × 10 <sup>3m</sup>	6.6 × 10 <sup>9n</sup>	2.6 × 10 <sup>6o</sup>

Modified from Young [16].

<sup>a</sup>Young [16].

<sup>b</sup>Bockris and Oldfield [44].

<sup>c</sup>Armstrong et al. [45].

<sup>d</sup>O<sub>2</sub> + e<sup>-</sup> → O<sub>2</sub><sup>•-</sup>.

<sup>e</sup>HO<sub>2</sub><sup>•</sup> + e<sup>-</sup> → HO<sub>2</sub><sup>-</sup>.

<sup>f</sup>HO<sub>2</sub><sup>•</sup> + e<sup>-</sup> + H<sup>+</sup> → H<sub>2</sub>O<sub>2</sub>.

<sup>g</sup>OH<sup>•</sup> + e<sup>-</sup> → OH<sup>-</sup>.

<sup>h</sup>OH<sup>•</sup> + e<sup>-</sup> + H<sup>+</sup> → H<sub>2</sub>O.

<sup>i</sup><sup>1</sup>Δ<sub>g</sub>O<sub>2(aq)</sub> + e<sup>-</sup> → O<sub>2</sub><sup>•-</sup>.

<sup>j</sup>Calculated using restricted open-shell HF (ROHF) using the PM7 method, see *Descriptor calculation*.

<sup>k</sup>Based on pH = 6.9, pKa = 4.9 and [I]<sub>ss</sub> ("steady-state" concentration) for O<sub>2</sub><sup>•-</sup> in the upper layer of surface waters.

<sup>l</sup>By Wardman [46].

<sup>m</sup>By Kozmér et al. [47].

<sup>n</sup>Luo et al. [48].

<sup>o</sup>Arnold et al. [49].

### Reductive pathway

In an attempt to explain the aforementioned outliers, data recorded at pH < 7 were excluded to limit the influence of HO<sub>2</sub><sup>•</sup> (which can react as an electrophile, instead of nucleophile). Since for polyphenols H-abstraction (i.e. oxidation) has been reported to be an important mechanism, compounds lacking functional groups other than phenols were excluded, and considered separately (see Section on "Oxidative pathway").

### Oxidative pathway

To investigate the relative importance of the oxidative pathway, we evaluated the relevance of  $E_{HOMO}$  to the rate constants obtained only at acidic conditions. Data were included for which pH ≤ 4.9 (in which HO<sub>2</sub><sup>•</sup> is the predominant speciation state). Data were also included when it was specifically stated "reaction with HO<sub>2</sub><sup>•</sup>." Apart from pH, no further selection based on chemical families was performed. Hence, (poly)phenols were included.

### Statistical analysis

Stepwise regression was used to select relevant descriptors and develop QSPRs. The coefficient of determination ( $R^2$ ), the residual sum of squares (rss), and probability values ( $p$ ) were calculated as indicators of the goodness of fit and correspondence of the relationship between descriptors and experimental data, respectively. All QSPRs were evaluated using leave-one-out cross-validation ( $Q^2_{LOOCV}$ ). External validation is important to determine the robustness and predictive capability of a QSPR [50]. In some

cases though, external validation can underestimate the predictive capability. Moreover, reserving a fraction of the data for external validation may be a waste of useful information. When only a limited amount of descriptors are used the statistics for the training and test set converge, irrespective of data partitioning and descriptors used [51]. To determine whether external validation is useful here (in addition to  $R^2$ , rss,  $p$  and  $Q^2_{LOOCV}$ ), we applied external validation to the oxidative model (data randomly split 80:20). In addition, we tested the QSPR (developed for acidic pH, ≤ 4.9), using data recorded at 4.9 ≤ pH ≤ 7.

## Results

### Reductive pathway

From the initial analysis (on the entire dataset, with an average pH of ~7, i.e. mostly reducing conditions),  $E_{LUMO}$  was found the most relevant descriptor (Supporting Information Figure S1(B)). Subsequently, the relationship was strengthened for the curated dataset (including only data for which pH ≥ 7). Illustratively, low values for  $E_{LUMO}$  were calculated for the highly conjugated fullerene C-60 (Figure 1), the carbonyl compound diphenoquinone (Supporting Information) and the powerful oxidant tetrani-tromethane (Figure 1). Conversely, high values were obtained for acetate (Figure 1) and tert-butyl hydroperoxide (Figure 1). These extreme values (-2.5 to +2.0 eV) mark the applicability domain of the QSPR developed (Equation (2)):

$$\log k_r O_2^{\bullet-} = -2.5 E_{LUMO} + 3.2 \quad (\text{pH} \geq 7) \quad (2)$$

$$N = 127, R^2 = 0.84, Q^2_{LOOCV} = 0.83,$$

$$p < 10^{-5}, \text{rss} = 19.78$$

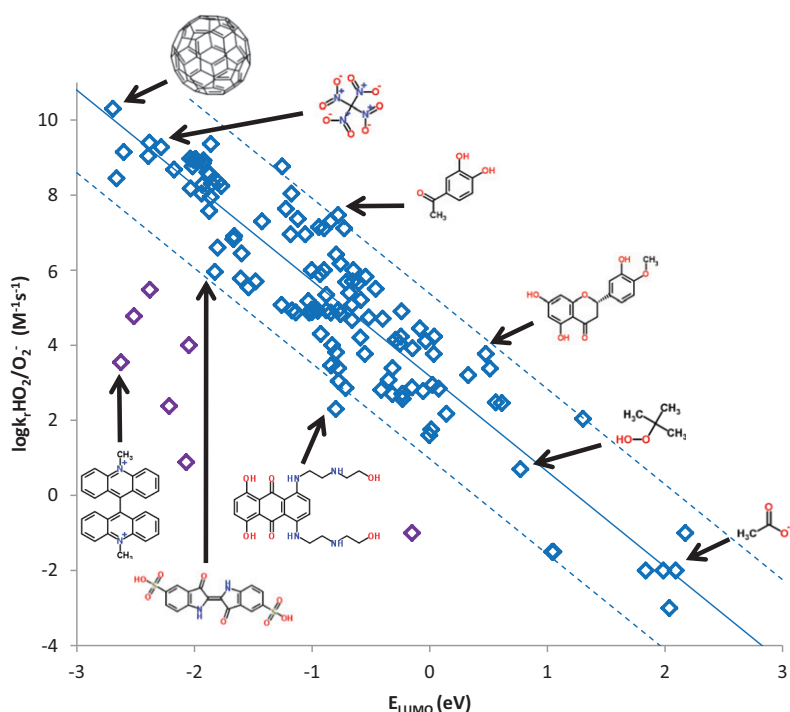


**Figure 1.** Relationship between the energy of the lowest unoccupied molecular orbital ( $E_{\text{LUMO}}$ ) and the bimolecular reaction rate constant with  $\text{O}_2^{\bullet-}$  (i.e. under reducing conditions,  $\text{pH} \geq 7$ ). The data shown exclude compounds with no functional groups other than phenols. Dashed lines indicate confidence levels of  $2\sigma$ . Purple data points denote aromatic cations (outliers). Structures shown indicate the applicability domain.

As mentioned above, aromatic cations (shown in purple in Figure 1) and compounds with only phenolic functional groups (excluded from Figure 1) were outliers and thus not included in derivation of the uni-parameter QSPR (Equation (2)). The uni-parameter model was established with satisfactory correlation ( $R^2 = 0.84$ ) and interpretability. Since no other descriptors were selected which significantly improved the model we discuss the outliers based on mechanistic grounds and propose additional chemical descriptors that may be screened as soon as more kinetic information becomes available (see Discussion).

### Oxidative pathway

Under oxidising conditions  $E_{\text{HOMO}}$  was identified as the most relevant descriptor for the reaction rate constant. Initially, only data recorded at  $\text{pH} \leq 4.9$  were included, analysis of which ascertained the oxidative nature of  $\text{HO}_2^{\bullet}$  (and relevance of  $E_{\text{HOMO}}$ ) under such conditions, Equation (3) (filled red symbols in Figure 2):

$$\begin{aligned} \log k_r \text{HO}_2^{\bullet} &= 2.1 E_{\text{HOMO}} + 22.9 \quad (\text{pH} \leq 4.9) \quad (3) \\ N &= 24, R^2 = 0.92, Q^2_{\text{LOOCV}} = 0.89, \\ p &< 10^{-5}, \text{rss} = 5.47 \end{aligned}$$

Subsequently, data recorded at pH up to 7 for non-phenols reacting via one-electron oxidation or addition was added. This significantly strengthened the relationship with  $E_{\text{HOMO}}$ . A high value for  $E_{\text{HOMO}}$  for

hydroethidine and a low value for DL-threonine corresponded to high and low rate constants, respectively (Figure 2). The extreme values for  $E_{\text{HOMO}}$  were  $-11.0$  to  $-8.0$  eV, and mark the applicability domain of the third QSPR developed, see Equation (4).

$$\begin{aligned} \log k_r \text{HO}_2^{\bullet}/\text{O}_2^{\bullet-} &= 1.7 E_{\text{HOMO}} + 19.9 \quad (\text{pH up to } 7) \quad (4) \\ N &= 46, R^2 = 0.92, Q^2_{\text{LOOCV}} = 0.91, \\ Q^2_{\text{ext}(9)} &= 0.98, p < 10^{-5}, \text{rss} = 1.91 \end{aligned}$$

Finally, compounds recorded at pH approximately 7 reacting via H-transfer were added (e.g. phenols), open black symbols in Figure 2. These compounds were notable outliers (higher rate constants than expected). For completion,  $E_{\text{HOMO}}$  was computed also for their deprotonated structures (filled black symbols, Figure 2).

## Discussion

### Reductive pathway

Rate constants for reduction by  $\text{O}_2^{\bullet-}$  increase when the difference between the energy of the singly occupied molecular orbital ( $E_{\text{SOMO}}$ ) of  $\text{O}_2^{\bullet-}$  and  $E_{\text{LUMO}}$  (of the organic singlet) decreases (e.g.  $E_{\text{LUMO}} = -2.7$  eV for fullerene C-60, Figure 1). The energy of the SOMO of  $\text{O}_2^{\bullet-}$  is approximately  $-4$  eV, as calculated empirically (Table 1). The slope of Equation (2) (i.e.  $2.5 \pm 0.1$  eV $^{-1}$ ) agrees well with previous results for radical reactions

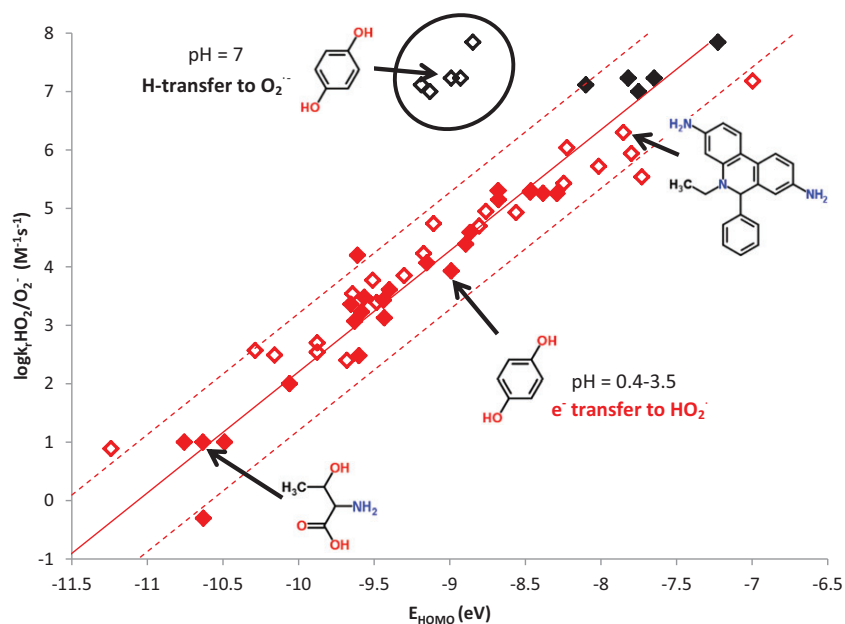


**Figure 2.** Relationship between the energy of the highest occupied molecular orbital ( $E_{\text{HOMO}}$ ) and the reaction rate constant with  $\text{HO}_2^\bullet$  and  $\text{HO}_2^\bullet/\text{O}_2^{\bullet-}$ , that is, under oxidising conditions ( $\text{pH} \leq 4.9$ , filled red) and including intermediate conditions ( $\text{pH}$  up to 7, open red). Open black symbols denote hydrogen abstraction (at  $\text{pH} \sim 7$ ). Upon deprotonation of the (poly)phenols, the calculated value for  $E_{\text{HOMO}}$  increases so that the data points (filled black) fall within the expected range (dashed lines,  $2\sigma$ ). Structures shown indicate the applicability domain.

involving many different hydrogen atom donors [52] which found 2.5–3 orders of magnitude difference in reactivity per eV. The dependence of  $k_r$  on these energy differences is attributable to frontier molecular orbital (FMO) interaction but may also result from the increasing polarisation, and concomitant stabilisation, of the transition state as the energy difference between the reactants decreases [53]. Based on considerations described in detail elsewhere [54,55] Klopman and Salem proposed a simplified formula for the energy change ( $\Delta E$ , and by extension  $k_r$ ), when two orbitals of two reactants (nucleophile and an electrophile) overlap (Equation (5)) [56]. Based on a constant value for  $E_{\text{SOMO}}(\text{O}_2^{\bullet-})$ ,  $E_{\text{LUMO}}$  would be inversely proportional to  $k_r$ :

$$\log k_r \sim -\frac{Q_{\text{nuc}} Q_{\text{elec}}}{\epsilon R} + \frac{2(\beta c_{\text{nuc}} c_{\text{elec}})^2}{E_{\text{HOMO,nuc}} - E_{\text{LUMO,elec}}} \quad (5)$$

*The coulombic term*      *The frontier orbital term*

In which  $\beta$  denotes the resonance integral and  $c_{\text{nuc}}$  and  $c_{\text{elec}}$  the atomic orbital coefficients on the nucleophile and electrophile, respectively. Full interpretation of results via Equation (5) would require accurate determination of the ESOMO for aqueous superoxide. However, it is noted that the value obtained (Table 1) is uncertain ( $\sim -4$  eV). Based on their relatively low  $E_{\text{LUMO}}$ , aromatic cations are prone toward nucleophilic attack, more so than simple benzenes, or even pyridines [57,58]. Looking at Figure 1, however, aromatic cations are notable outliers (purple data points). Their

relatively low reactivity may be the result of several effects, not accounted for in the descriptor calculation or in the theoretical assumptions made (Equation (5)). Firstly, solvent  $\text{H}_2\text{O}$  molecules may interact with the aromatic cation via  $\text{lp}-\pi$  interaction [33,59,60]. In  $\text{lp}-\pi$  interactions, the HOMO of the molecule bearing the lone pair and LUMO of the  $\pi$  moiety are concerned, and their gap substantially affects the interaction energy. A positive charge on a heteroaromatic molecule can enhance the magnitude of the  $\text{lp}-\pi$  interaction energy, more so than for neutral compounds [61]. This effect may be inadequately covered via the conductor-like screening (COSMO) approximation for water in the derivation of QM descriptors (see Methods) [40,41]. Illustratively, Scheiner et al. found that the  $\text{lp}-\pi$  interaction energy of a water–imidazole complex will increase by protonation of the imidazole moiety [62]. For lucigenin (Figure 1) specifically, the redox equilibrium is solvent dependent, with polar solvents inhibiting the rate constant [63]. Second, nucleophilic attack by  $\text{O}_2^{\bullet-}$  may result in a considerable relocalization of charges in the aromatic molecule. This is not accounted for by Equation (5), hence a specific term for delocalisation and bonding-like interactions in the transition state may be needed. In analogy, a distinction between inner-sphere and outer-sphere mechanisms could be useful. The structural variability of the compounds investigated falls within the Marcus “normal” region (rate constants

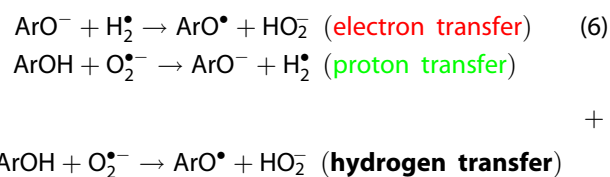
increase with higher  $\Delta E$ , i.e. when orbital energies are similar). Apparently activation energies are relatively low as compared with  $\Delta E_{\text{FMO}}$  or depend heavily on  $\Delta E_{\text{FMO}}$  themselves, but this may not apply to aromatic cations. Third, steric and geometric effects might play a role because  $\text{O}_2^{\bullet-}$ , and/or  $\text{H}_2\text{O}$  solvent molecules would need to be able to approach the empty  $\pi^*$  orbital. Ring flattening is known to affect the LUMO energy [58,63], and HOMO/LUMO transitions have been associated with the dihedral angle between aromatic planes [64]. Coulombic interaction between the reagents is not expected to lower the rate constant since the charge of aromatic cations is opposite to that of  $\text{O}_2^{\bullet-}$  which would only promote the reaction (first term in Equation (5)). Lastly, in order for a reduction reaction to proceed, the symmetry of overlapping orbitals should be the same (antisymmetric, e.g. in the case of carbonyl species) [53].

Compounds with notable deviation from Equation (2) (lower  $k_r$  than expected, but not necessarily outliers) include mitoxantrone and indigodisulfonate (Figure 1). For compounds such as these, intramolecular H-bonding,  $\text{XH}-\pi$ ,  $\text{lp}-\pi$  and  $\pi-\pi$  interactions may be involved [62,65,66]. As compounds containing no functional groups other than phenols were excluded from the QSPR building (outliers in Equation (2), see Supporting Information), it should be no surprise that the  $\text{ArOH}$ -containing compounds are among the ones deviating from Equation (2) (Figure 1), see also the combined model in Figure 3. Hesperetin and 3,4-dihydroxyacetophenone have higher values than expected, possibly also due to H-bonding. It is noted that H-bonding has been used to describe H-abstraction (i.e. oxidation) reactions of phenolic antioxidants [67,68]. Variability in the experimental pH causes some of the variance in the reductive model, for example, in cases when the  $\text{pK}_a$  of the compounds is unknown (i.e. predicted) or the experimental system is not buffered (as is also expected for the oxidative model), see also Figure 3. However, the hydrogen-donating capacity of  $\text{HO}_2^{\bullet}$  is likely not an issue [69] because only data for which  $\text{pH} > 7$  was included, that is, extent of protonation of  $\text{O}_2^{\bullet-}$  is low.

### Oxidative pathway

As the difference between  $E_{\text{SOMO}}$  ( $\text{HO}_2^{\bullet}$ ,  $\sim -6$  eV) and  $E_{\text{HOMO}}$  (organic singlet) decreases, the rate constant for oxidation by  $\text{HO}_2^{\bullet}$  (or  $\text{O}_2^{\bullet-}$ ) increases. This is illustrated for hydroethidine and threonine, being the far-right and far-left data points in Figure 2. Under oxidising conditions ( $\text{pH} < 4.9$ ), the QSPR for  $k_r(\text{HO}_2^{\bullet})$  developed had good statistics (Equation (3)). As

might be expected, external validation ( $N=9$ ,  $Q^2_{\text{test}}=0.98$ ) did not provide additional information on the performance of the uni-parameter models (Equation (4)) although it confirmed their predictive capabilities (see Supporting Information). Analogous to the reductive pathway, the high correlation can be attributed to FMO interaction [53]. The QSPR developed for reaction with  $\text{HO}_2^{\bullet}/\text{O}_2^{\bullet-}$  under intermediate conditions ( $\text{pH}$  up to 7) also had good statistics ( $R^2=0.95$ ), but only when excluding H-donor molecules (i.e. (poly)phenols) measured at  $\text{pH}$  approximately 7 (Figure 2). For instance, the rate constant measured for hydroquinone at  $\text{pH}$  approximately 7 is over 3 orders of magnitude higher than expected on the basis of Equation (3). Interestingly though, when  $E_{\text{HOMO}}$  is computed for the anionic form of hydroquinone the data fell within the expected range (filled black symbols in Figure 2), even though the  $\text{pK}_a$  of hydroquinone is only approximately 10. The  $\Delta E_{\text{HOMO}}$  for hydroquinone/(mono-)deprotonated hydroquinone is 2 eV which would imply a 3–4 orders difference in  $k_r$ , according to Equation (3), which matches the experimental values for hydroquinone ( $\log k_r=7.2$  and 3.9) obtained at neutral and at acidic  $\text{pH}$ , resp. For (poly)phenols such as hydroquinone, H-abstraction has been established to be the dominant pathway for reaction with  $\text{O}_2^{\bullet-}$  [70]. Concomitantly, H-abstraction by  $\text{O}_2^{\bullet}$  may result in the same product as in case of electron transfer by  $\text{HO}_2^{\bullet}$ , Equation (6):



Previously, the rate of hydrogen abstraction by 23 structurally different, positively-charged aryl radicals has been correlated with the (calculated) vertical electron affinities (EA) of aryl radicals [52] ( $\text{EA} \sim$  negative of  $E_{\text{LUMO}}$ ). Conversely, the vertical ionisation energies of hydrogen-atom donors were found to play an important role. It is also noted that the protonation of  $\text{O}_2^{\bullet-}$  by a free proton is diffusion limited:  $5\text{--}7.2 \times 10^{10} \text{ M}^{-1} \text{ s}^{-1}$  (for  $2 \leq \text{pH} \leq 4$ ), that is, not rate limiting [30]. It is, therefore, to be expected that, as a general rule, H-abstraction by  $\text{O}_2^{\bullet-}$  is related to the energy of the HOMO. Based on this, the calculation of  $E_{\text{HOMO}}$  for the deprotonated structure might be justified, in order to compare the data for hydrogen transfer reactions to reactions involving (rate limiting) electron transfer only. When the deprotonated structures are included in Equation (3) (closed black symbols in Figure 2) the

upper limit of the applicability domain for the QSPR for  $k_r(\text{HO}_2^\bullet)$  increases from  $-8.5$  to  $-7.5$  eV.

In the case of phenols, hydrogen transfer is expected at the O–H bond. However, an O–H bond itself might be part of the HOMO. Hence, bond dissociation energies (BDE) for simple phenols (and other congenic series) have been correlated to  $E_{\text{HOMO}}$  as well as antioxidant activity [67]. Many other chemicals families are known to participate in H-abstraction such as sulphides [71,72], pyrroles [73] and benzylic C–H bonds [74]. Generally, if the BDE is lower than the BDE of the OO–H bond of hydroperoxyl, the reaction is favoured ( $\sim 344$ ,  $368$  and  $377$   $\text{kJ mol}^{-1}$  for 4-HOC<sub>6</sub>H<sub>4</sub>O–H, HOO–H and ROO–H, respectively, in DMSO [75]). Reaction rates are generally relatable to BDE [66]. However, analysis using the BDE of structurally different H-donors (X–H, with X being any heavy atom) did not reveal a significant correlation [52]. Apparently the relevance of BDE depends on the type of hydrogen-atom donor. It is known that an anionic charge can cause a dramatic weakening of an adjacent C–H bond [76], and even small variations in BDE may be associated with large variations in rate constants. In contrast to a concerted mechanism, stepwise H-abstraction may first involve rate-limiting proton transfer to superoxide, with the deprotonated structure subsequently undergoing fast oxygenation [77,78]. Therefore, BDE is only a primary descriptor for a rough estimate of the kinetics. For a better estimate of the kinetics, a more thorough knowledge of the oxidative scavenging mechanism is required [66]. For complex (poly)phenols a combination of descriptors such as  $E_{\text{HOMO}}$ ,  $\text{pK}_a$ , BDE, hydrogen bonding, as well as geometrical descriptors may be needed [67,68,79]. For example, the  $\text{pK}_a$ 's of hydroquinone are indicators of the electron density (e.g. the lower the  $\text{pK}_a$ , the less stable to autoxidation) [80] (Figure 2).

Varying the pH may not only affect the protonation state of the organic chemical, but it also changes the reduction potential of the superoxide (Table 1). The difference in  $E_{\text{SOMO}}$  between  $\text{HO}_2^\bullet$  and  $\text{O}_2^{\bullet-}$  is approximately 2 eV (Table 1). When treating the SOMO of  $\text{HO}_2^\bullet/\text{O}_2^{\bullet-}$  as the electron accepting orbital, a “relative” rate constant may be calculated based on this energy difference and Equation (1):  $\log k_r(\text{rel.}) = \sim 5$ . This would imply a 5 orders of magnitude decrease in the observed oxidation rate constant upon deprotonation of  $\text{HO}_2^\bullet$ . This agrees with experimental values of  $1.18 (\pm 0.20) \times 10^3$  and  $1 \times 10^{-2} - 1 \times 10^{-1} \text{ M}^{-1} \text{ s}^{-1}$  reported for the reaction of linoleic acid with  $\text{HO}_2^\bullet$  and  $\text{O}_2^{\bullet-}$ , respectively (i.e. 4–5 orders of magnitude difference) [30]. Hence, for reactive functional groups with  $\text{pK}_a$  or  $\text{pK}_b \ll \text{pH}$  the dependence of the oxidative reaction rate ( $k_r$ ,  $\text{HO}_2^\bullet/\text{O}_2^{\bullet-}$ ) on pH is due to  $E_{\text{SOMO}}$  changes upon (de)protonation of the

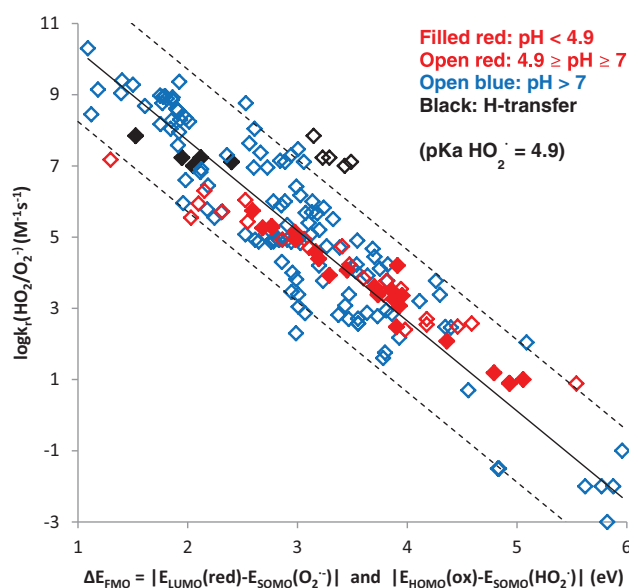


**Figure 3.** Relationship between  $|E_{\text{LUMO}}(\text{red}) - E_{\text{SOMO}}(\text{O}_2^{\bullet-})|$ ,  $|E_{\text{HOMO}}(\text{ox}) - E_{\text{SOMO}}(\text{HO}_2^\bullet)|$  and the bimolecular  $\text{HO}_2^\bullet$  (red) and  $\text{O}_2^{\bullet-}$  (blue) reaction rate constant. Open black symbols indicate hydrogen abstraction at  $\text{pH} \sim 7$ . The solid line is a linear fit to all the data excluding outliers from Figure 1, and the dashed lines indicate confidence intervals of  $2\sigma$ .

oxidant. As noted, for compounds with relevant (de)protonable groups such as (poly)phenols the apparent  $k_r$  may increase at higher pH due to H-transfer. However, H-transfer cannot explain the kinetic data for (poly)phenols at extreme (alkaline) pH. In such cases there is no (weak) phenolic proton to be abstracted by the  $\text{O}_2^{\bullet-}$  (see also Figure 4), and  $\log k_r$  for oxidation should decrease according to the lower reduction potential for  $\text{O}_2^{\bullet-}$  compared with  $\text{HO}_2^\bullet$  (Table 1; Equation (4)). The other way around, literature indicates that  $\text{HO}_2^\bullet$  is rather feeble with regard to H-abstraction, as compared with other oxidants [69], which explains the strong correlation at acidic pH ( $< 4.9$ ) (Figure 2). These competing effects may be the reason for local optima in  $\text{HO}_2^\bullet/\text{O}_2^{\bullet-}$  rate constants for certain compounds [21,30,81,82], for example, for ascorbic acid as found by Nadezhdin and Dunford (1979) [82].

### Competition kinetics and pathway analysis

According to FMO theory, the difference between  $E_{\text{LUMO}}$  and  $E_{\text{HOMO}}$  is the most important parameter describing the rate of electron transfer, irrespective of the reaction coordinate (direction of electron flow). For this reason, Figure 3 shows both oxidation and reduction rate constants (from Figures 1 and 2) versus the difference between  $E_{\text{LUMO}}$  (organic singlet) and  $E_{\text{SOMO}}$  ( $\text{O}_2^{\bullet-}$ ), as well as between and  $E_{\text{HOMO}}$  (organic singlet)

and  $E_{\text{SOMO}}(\text{HO}_2^\bullet)$ . Doing so, we visualise the SOMO of  $\text{HO}_2^\bullet/\text{O}_2^{\bullet-}$  as both the electron donating (blue) and accepting (red) orbital.

The combined model yields proper statistics ( $R^2 = 0.84$ ,  $N = 170$ , Figure 3). Some of the (poly)phenols identified as outliers in Figure 2 might be explained in terms of the combined model, which has a (log) standard deviation (SD) of  $1.0 \text{ M}^{-1} \text{ s}^{-1}$  (1.1 and 0.5 for the reductive and oxidative model, resp.). However, when correcting for protonation (Equation (6)) the experimental values are fully within the expected range (dashed lines in Figure 3). Organic cations remain outliers (see *Reductive pathway* section). From Figure 3 it may be noted that the dependence (i.e. slope) of  $k_r$  on  $\Delta E_{\text{FMO}}$  for reduction ( $2.5 \pm 0.1 \text{ eV}^{-1}$ ) is greater than that for oxidation ( $2.1 \pm 0.1 \text{ eV}^{-1}$ ), although the residual variance for the regression is high (blue symbols) and experimental pH is highly variable (open red symbols). Based on the Salem–Klopman equation (Equation (5)) however, there should be no difference in the slopes between the regressions of  $|E_{\text{LUMO}} - E_{\text{SOMO}}(\text{O}_2^{\bullet-})|$  and  $|E_{\text{HOMO}} - E_{\text{SOMO}}(\text{HO}_2^\bullet)|$  (Figure 3) when considering equal heterogeneity in chemical structure. Nevertheless, the simultaneous incorporation of multiple experimental pH, functional groups and reaction pathways may affect the overall dependence on  $\Delta E_{\text{FMO}}$ . Obviously, since both a reductive and oxidative pathway may be possible for one chemical one needs to determine both  $|E_{\text{LUMO}} - E_{\text{SOMO}}(\text{O}_2^{\bullet-})|$  and  $|E_{\text{HOMO}} - E_{\text{SOMO}}(\text{HO}_2^\bullet)|$ . Even though this increases the computational time needed it may provide valuable mechanistic information, since the relative importance of the competing pathways may be determined. We stress that experiments involving superoxide and organic chemicals are inherently complex due to competing reductive and oxidative pathways. Speciation of the organic chemical as function of the pH further increases the complexity. Nevertheless, disentanglement of speciation states, reaction pathways, and other factors can help to develop a robust model (Figure 4). This may be particularly useful when one needs to distinguish between the simultaneous influence of pH on both the oxidant and reductant. As mentioned,  $\text{O}_2^{\bullet-}$  can react with H-donors (i.e. (poly)phenols) via H-abstraction (top left arrow in Figure 4). However, we note again that the hydroperoxyl radical ( $\text{HO}_2^\bullet$ ) can also behave as a hydrogen-donor molecule (dashed bottom-right arrow in Figure 4), due to its weak O–H bond (49 kcal/mol) [69]. This phenomenon is expected to occur primarily at acidic pH ( $\text{pH} < 4.9$ ) at which it may compete with one-electron oxidation.

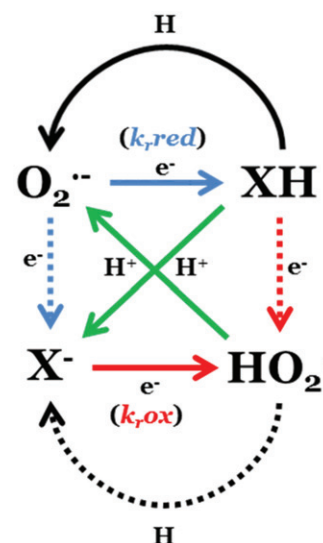


**Figure 4.** Possible flows for proton transfer (green) and electron transfer (blue/red) between superoxide ( $\text{O}_2^{\bullet-}/\text{HO}_2^\bullet$ ) and an organic molecule ( $\text{XH}/\text{X}^-$ ). The solid blue and red arrows correspond to the data in Figure 1 (reduction) and Figure 2 (oxidation), respectively. Black arrows denote hydrogen transfer (i.e. combined proton and electron transfer). The importance of H-transfer is related to the relative BDE of X–H.

#### Limitations, implications and outlook

As with any empirical model, the quality of the data heavily affects the strength of the relationships and confidence in predictions made therewith. The data used in this study originates from different methods. Hence, varying quality and systematic differences may be expected. Matrix or temperature effects may have played a role, such as reaction or complexation with metal impurities (e.g. copper), interaction with buffering agents, or ionic strength impacts in general. Ideally rate constants extrapolated to zero ionic strength should be used, but this requires detailed mechanistic information that is commonly lacking. To exclude the involvement of metal cations, chelating agents are useful, but not uniformly applied. Also, side reactions may have occurred involving, for example, the solvated electron or the hydroxyl radical in case of improper quenching. These issues may be especially pronounced for data acquired using competition kinetics, which is inherently less reliable [30]. The majority of the data, however, was generated using pulse radiolysis and flash photolysis, which are somewhat similar techniques [30,34]. For example, a factor 1.4 difference was found for the  $k_r$  of Cytochrome C measured using pulse radiolysis ( $k_r = 8.0 \times 10^5$ ,  $\text{pH} = 7.2$ , using either *tert*-butanol or glycerol as  $\text{OH}^\bullet$  scavenger) and flash photolysis ( $k_r = 5.84 \times 10^5$ ,  $\text{pH} = 7.3$ , using tetramethylethylenediamine, EDTA and FMN) [30]. A difference of “only” a factor of 1.8 was reported for a dioxouranium(VI)–hydroperoxy

complex measured using pulse radiolysis and electron paramagnetic resonance ( $k_r = 5 \times 10^5$ , and  $9.0 \times 10^5$ ), respectively [30]. Hence, the quality of the data (uncertainty  $<0.3$  in log units) is not expected to influence the relationships developed in this study, and the data is not over-fitted.

The models developed in this study (Equations (2–4)) should be utilised only for chemicals for which the models are parameterised. As noted in the *Methods* section, we made no prior distinction between chemicals; which were diverse including polycyclic aromatics, halogenated aromatics, carboxylic acids, enes, quinones, phenols/phenolates, ethers, aldehydes, thiols, arylamines, aliphatic amines, peptides, N–O bonds and N–X (halogen) bonds. For polyphenols and other compounds with weak R–H bonds, for example,  $<377 \text{ kJ mol}^{-1}$  (flexible, multi- and poly-functional chemicals in general) predictions for  $k_r(\text{O}_2^{\bullet-})$  are possible, but more accurate values can be obtained using additional descriptors accounting for intramolecular interaction, competing reaction pathways and speciation. Illustratively, for theaflavin (a well-known polyphenolic antioxidant, with  $\text{pK}_a \sim 6$ )  $\log k_r(\text{O}_2^{\bullet-})$  values of  $5.5(\pm 1.1)$ ,  $5.9(\pm 0.5)$  and  $7.3(\pm 1.0)$  can be derived for one-electron reduction, one-electron oxidation and H-transfer, respectively (the latter upon deprotonating its structure, see Equation (6)) (using Equations (2) and (3)). The experimental value, approximately 7 [66] indicates that H-transfer is the dominant pathway at neutral conditions, but this may be different at other pH which can affect the protonation state as well as intramolecular interaction. For larger molecules with multifunctional groups intramolecular H-transfer could be relevant, especially when information on the reaction product is desired. This study does not necessarily consider compounds with multiple weak X–H bonds which may extend the number of possible pathways, and additional descriptions that would be needed [83]. Moreover, H-transfer can occur via proton-coupled electron transfer (PCET), hydrogen atom transfer (HAT), or electron proton transfer (EPT), each with different characteristics [66,84–86]. Tautomerization (e.g. for keto-enols [87] and halogen-substituted amides [88]) should be accounted for by establishing the most stable isomer. In turn, highly captodative molecules might not be accurately described by our method because delocalisation in the transition state needs to be taken into account. Better results might be achievable using ab-initio methods (i.e. density functional theory) but these are computationally demanding, especially for large, flexible structures. Hybrid methods (e.g. combined quantum mechanics/molecular mechanics) may be

suitable to study large molecules, especially when the electrostatic effect of water molecules is to be incorporated (i.e. aromatic cations, see above). Lastly, there is an increasing need to quantify the contribution of tunnelling [86]. Often observed for (but not limited to) phenolic antioxidants, tunnelling reduces the apparent Arrhenius activation energy of electron or H-transfer reactions. Tunnelling is dependent on the conformation and compactness of the transition state, the energy landscape and thermal fluctuations [65,89], and can theoretically increase the apparent rate up to several orders of magnitude [89,90].

Importantly, Equations (2–4) should not be applied to radical intermediates, stabilised radicals, or compounds containing significant “radical character,” such as proxyls and verdazyls [91,92] because of the empirical nature of the method. Obviously, this study also does not consider metal-containing complexes (e.g. predicted values for  $\log k_r(\text{HO}_2^{\bullet})$  of ferro(II)cyanide and bis(histidinato)copper(II) of 6.2 and 6.3 ( $\pm 0.5$ ) versus experimental values of 4.8 and 8.5, see Supporting Information). For one, a coordinating metal ion may lower the electron density of the reactive centre, or it may participate in redox reactions itself (especially when d-electrons are involved). Whereas aliphatic cations were included, aromatic cations were shown to be systematic outliers (as discussed previously), and hence fall outside of the applicability domain. Though our models are parameterised toward organic molecules, the reaction site can involve a heteroatom (O, S, N, etc.). Based on this, the relationships might be useful for fully inorganic molecules as well. For example, predicted and experimental values for  $\log k_r(\text{O}_2^{\bullet-})$  of  $\text{H}_2\text{O}_2$  are  $1.4(\pm 1.1)$  and 0.3, respectively, and for molecular bromine ( $\text{Br}_2$ ) being  $9.0(\pm 1.1)$  and 9.7, respectively. However, higher uncertainty needs to be anticipated as illustrated by predicted and experimental values for  $\log k_r(\text{O}_2^{\bullet-})$  of ozone being  $6.4(\pm 1.1)$  and 9.2, respectively.

The study may be useful to explain the kinetics for related oxidants as well. For example, the hydroxyl radical ( $\text{OH}^{\bullet}$ ) is generally more reactive than  $\text{HO}_2^{\bullet}$  as is indicated by their reduction potential (Table 1). Considering the SOMOs of  $\text{OH}^{\bullet}$  and  $\text{HO}_2^{\bullet}$  as the electron accepting orbitals, one can predict a relative rate constant of  $10^5$ – $10^6$  (i.e. 5–6 orders of magnitude faster reaction with  $\text{OH}^{\bullet}$ , compared with  $\text{HO}_2^{\bullet}$ ) using their energy difference (2.3 eV) and Equations (2 and 3). This value is in line with experimentally derived values for  $k_r$  of  $2.7 \times 10^3$  and  $1 \times 10^{10}$  (for  $\text{HO}_2^{\bullet}$  and  $\text{OH}^{\bullet}$ , respectively) for phenol, that is, approximately 6.5 orders of

magnitude difference (Table 1). Such derivations should be considered rough estimates though, since the reaction coordinate and geometry of transition states can vastly differ between oxidants [93]. Moreover, hydration and coulombic forces need to be taken into account, which are reagent-specific [94]. Also,  $\text{OH}^\bullet$  is more likely to react via H-abstraction than is  $\text{HO}_2$ . For more accurate cross-radical predictions electrode potentials could be used. Such information is available [45], even for complex redox couples such as the iron-oxo species present in oxidising P450 enzymes [95].

Anti-oxidant activity in *in vitro* assays has often been explained in terms of lipophilicity, for example, through the octanol–water partitioning coefficient [22,96]. From this, it is clear that not solely the radical quenching capacity, but also bioavailability is relevant for complex biological systems. Moreover, certain anti-oxidants may act as competitive inhibitors of ROS-generating enzymes or oxidative signal transducers. Nevertheless, we feel that the relationships derived in this study are useful to initiate the description and explanation of electron transfer involving superoxide. By extension, many phenomena observed in biology, synthetic photochemistry and environmental science can be better understood. We also feel that we alleviated some of the previous difficulties with applying QSPR to describe the reactivity of non-congeneric chemicals with superoxide. Further model refinement and extension to more complex molecules may require flexible and non-linear algorithms and additional quantum chemical descriptors using semi-empirical MO theory.

## Acknowledgements

The authors wish to thank Prof. Dr. Hendriks for fruitful discussions.

## Disclosure statement

The authors declare that they have no conflicts of interest.

## References

- [1] Grusschow S, Sherman DH. Chapter 10: The biosynthesis of epoxides. In: Yudin AK, editor. Aziridines and epoxides in organic synthesis. Weinheim (Germany): Wiley-VCH Verlag GmbH; 2006. p. 349–351.
- [2] Budanur BM, Khan FA. Superoxide chemistry revisited: synthesis of tetrachloro-substituted methylenenortricyclenes. *Beilstein J Org Chem*. 2014;10:2531–2538.
- [3] Hayyan M, Hashim MA, AlNashef IM. Superoxide ion: generation and chemical implications. *Chem Rev*. 2016;116:3029–3085.
- [4] Jiang WQ, Zhang XQ, Sui ZH. Potassium superoxide as an alternative reagent for Winterfeldt oxidation of beta-carbolines. *Org Lett*. 2003;5:43–46.
- [5] Scully FE, Davis RC. Superoxide in organic synthesis: a new mild method for the oxidation of amines to carbonyls via N-chloramines. *J Org Chem*. 1978;43:1467–1468.
- [6] Singh KN. Mild and convenient synthesis of organic carbamates from Amines and carbon dioxide using tetraethylammonium superoxide. *Synth Commun*. 2007;37:2651–2654.
- [7] Kim YH, Lim SC, Kim KS. Activation of superoxide – application of peroxy-sulphur intermediates to organic-synthesis. *Pure App Chem*. 1993;65:661–666.
- [8] Tobiszewski M, Namieśnik J. Greener organic solvents in analytical chemistry. *Curr Opin Green Sustain Chem*. 2017;5:1–4.
- [9] De Grey ADNJ.  $\text{HO}_2^\bullet$ : the forgotten radical. *DNA Cell Biol*. 2002;21:251–257.
- [10] Muriel P. Liver pathophysiology: therapies and antioxidants. San Diego (CA): Academic Press; 2017.
- [11] Imlay JA, Fridovich I. Assay of metabolic superoxide production in *Escherichia-Coli*. *J Biol Chem*. 1991;266:6957–6965.
- [12] Benigni R. Quantitative Structure-Activity Relationship (QSAR) models of mutagens and carcinogens. Boca Raton (FL): CRC Press; 2003.
- [13] Rose AL, Moffett JW, Waite TD. Determination of superoxide in seawater using 2-methyl-6-(4-methoxyphenyl)-3,7-dihydroimidazo[1,2-a]pyrazin-3(7H)-one chemiluminescence. *Anal Chem*. 2008;80:1215–1227.
- [14] Hansard SP, Vermilyea AW, Voelker BM. Measurements of superoxide radical concentration and decay kinetics in the Gulf of Alaska. *Deep-Sea Res Part 1 Oceanogr Res Pap*. 2010;57:1111–1119.
- [15] Fujii M, Otani E. Photochemical generation and decay kinetics of superoxide and hydrogen peroxide in the presence of standard humic and fulvic acids. *Water Res*. 2017;123:642–654.
- [16] Young MA. Environmental photochemistry in surface waters. In: Lehr JH, Keeley J, editors. *Water encyclopedia: oceanography; meteorology; physics and chemistry; water law; and water history, art, and culture*. New York: Wiley and Sons; 2005.
- [17] Heller MI, Croot PL. Kinetics of superoxide reactions with dissolved organic matter in tropical Atlantic surface waters near Cape Verde (TENATSO). *J Geophys Res Oceans*. 2010;115:C12038.
- [18] Khlebnikov AI, Schepetkin IA, Domina NG, Kirpotina LN, Quinn MT. Improved quantitative structure-activity relationship models to predict antioxidant activity of flavonoids in chemical, enzymatic, and cellular systems. *Bioorg Med Chem*. 2007;15:1749–1770.
- [19] Sivakumar PM, Prabhakar PK, Doble M. Synthesis, antioxidant evaluation, and quantitative structure-activity relationship studies of chalcones. *Med Chem Res*. 2011;20:482–492.
- [20] Erzincan P, Saçan MT, Yüce-Dursun B, Danış Ö, Demir S, Erdem SS, Ogan A. QSAR models for antioxidant activity of new coumarin derivatives. *SAR QSAR Environ Res*. 2015;26:721–737.

- [21] Jovanovic SV, Steenken S, Tosic M, Marjanovic B, Simic MG. Flavonoids as antioxidants. *J Am Chem Soc.* 1994;116:4846–4851.
- [22] Pisoschi AMN. Methods for total antioxidant activity determination: a review. *Biochem Anal Biochem.* 2011; 247:237–241.
- [23] Ray S, Sengupta C, Roy K. QSAR modeling of antiradical and antioxidant activities of flavonoids using electrotopological state (E-State) atom parameters. *Cent Eur J Chem.* 2007;5:1094–1113.
- [24] Bendary E, Francis RR, Ali HMG, Sarwat MI, El Hady S. Antioxidant and structure–activity relationships (SARs) of some phenolic and anilines compounds. *Ann Agric Sci.* 2013;58:173–181.
- [25] Sun C, Zeng Y, Xu B, Meng L. Mechanism and kinetics for the reactions of methacrolein and methyl vinyl ketone with HO<sub>2</sub> radical. *New J Chem.* 2017;41: 7714–7722.
- [26] Mujika JI, Matxain JM. Theoretical study of the pH-dependent antioxidant properties of vitamin C. *J Mol Model.* 2013;19:1945–1952.
- [27] Sjöberg L, Eriksen TE, Révész L, Sjöberg L, Revesz L. The reaction of the hydroxyl radical with glutathione in neutral and alkaline aqueous-solution. *Radiat Res.* 1982;89:255–263.
- [28] Yin G, Danby AM, Kitko D, Carter JD, Scheper WM, Busch DH. Oxidative reactivity difference among the metal oxo and metal hydroxo moieties: pH dependent hydrogen abstraction by a manganese(IV) complex having two hydroxide ligands. *J Am Chem Soc.* 2008; 130:16245–16253.
- [29] Bonneau R, Violet P. F d, Jousot-Dubien J. Mechanism of photoreduction of thiazine dyes by EDTA studied by flash-photolysis.2. pH-dependence of electron abstraction rate constant of dyes in their triplet-state. *Photochem Photobiol.* 1974;19:129–132.
- [30] Bielski BHJ, Cabelli DE, Arudi RL, Ross AB. Reactivity of HO<sub>2</sub>/O<sub>2</sub> radicals in aqueous-solution. *J Phys Chem Ref Data.* 1985;14:1041–1100.
- [31] Abreu RMV, Ferreira ICFR, Queiroz MJRP. QSAR model for predicting radical scavenging activity of di(hetero)arylamines derivatives of benzo[b]thiophenes. *Eur J Med Chem.* 2009;44:1952–1958.
- [32] National Institute of Standards and Technology (NIST). NDRL/NIST Solution Kinetics Database on the Web. NIST Standard Reference Database 40; 2002. Available from: <http://kinetics.nist.gov/solution/>
- [33] Nolte TM, Peijnenburg WJGM. Aqueous-phase photooxygenation of enes, amines, sulfides and polycyclic aromatics by singlet (a<sup>1</sup>Δ<sub>g</sub>) oxygen: prediction of rate constants using orbital energies, substituent factors and quantitative structure–property relationships. *Environ Chem.* 2017;14:442–450.
- [34] Truscott TG. Pulse radiolysis and flash photolysis. In: Ricklis E, editor. *Photobiology.* Boston (MA): Springer; 1991.
- [35] ChemAxon, Calculator Plugin for structure property prediction. MarVin Version 5.2.0. Available from: [https://chemaxon.com/marvin-archive/5\\_2\\_0/marvin/](https://chemaxon.com/marvin-archive/5_2_0/marvin/)
- [36] Lee AC, Crippen GM. Predicting pK<sub>a</sub>. *J Chem Inf Model.* 2009;49:2013–2033.
- [37] Liao CZ, Nicklaus MC. Comparison of nine programs predicting pk(a) values of pharmaceutical substances. *J Chem Inf Model.* 2009;49:2801–2812.
- [38] O’Boyle NM. Open babel: an open chemical toolbox. *J Cheminform.* 2011;3:33.
- [39] Stewart JJP. Optimization of parameters for semiempirical methods VI: more modifications to the NDDO approximations and re-optimization of parameters. *J Mol Model.* 2013;19:1–32.
- [40] Stewart JJP. MOPAC. Colorado Springs (CO): Stewart Computational Chemistry; 2016.
- [41] Klamt A, Schuurmann G. Cosmo – a new approach to dielectric screening in solvents with explicit expressions for the screening energy and its gradient. *J Chem Soc Perkin Trans.* 1993;2:799–805.
- [42] Cao D-S, Xu Q-S, Hu Q-N, Liang Y-Z. ChemoPy: freely available python package for computational biology and chemoinformatics. *Bioinformatics.* 2013;29: 1092–1094.
- [43] Behar D, Czapski G, Rabani J, Dorfman LM, Schwarz HA. Acid dissociation constant and decay kinetics of the perhydroxyl radical. *J Phys Chem.* 1970;74: 3209–3213.
- [44] Bockris JO, Oldfield LF. The oxidation-reduction reactions of hydrogen peroxide at inert metal electrodes and mercury cathodes. *Trans Faraday Soc.* 1955;51: 249–259.
- [45] Armstrong DA, Huie RE, Koppenol WH, Lyman SV, Merényi G, Neta P, et al. Standard electrode potentials involving radicals in aqueous solution: inorganic radicals (IUPAC Technical Report). *Pure Appl Chem.* 2015; 87:1139–1150.
- [46] Wardman P. Reduction potentials of one-electron couples involving free-radicals in aqueous-solution. *J Phys Chem Ref Data.* 1989;18:1637–1755.
- [47] Kozmer Z. Determination of the rate constant of hydroperoxyl radical reaction with phenol. *Radiat Phys Chem.* 2014;102:135–138.
- [48] Luo X, Yang X, Qiao X, Wang Y, Chen J, Wei X, Peijnenburg WJGM. Development of a QSAR model for predicting aqueous reaction rate constants of organic chemicals with hydroxyl radicals. *Environ Sci Processes Impacts.* 2017;19:350–356.
- [49] Arnold WA, Oueis Y, O’Connor M, Rinaman JE, Taggart MG, McCarthy RE, et al. QSARs for phenols and phenolates: oxidation potential as a predictor of reaction rate constants with photochemically produced oxidants. *Environ Sci Processes Impacts.* 2017;19:324–338.
- [50] Golbraikh A, Tropsha A. Beware of q<sup>2</sup>! *J Mol Graph Model.* 2002;20:269–276.
- [51] Talevi A. Optimal partition of datasets of QSPR studies: a sampling problem. *Match Commun Math Comput Chem.* 2010;63:585–599.
- [52] Jing L, Nash JJ, Kenttämaa HI. Correlation of hydrogen-atom abstraction reaction efficiencies for aryl radicals with their vertical electron affinities and the vertical ionization energies of the hydrogen-atom donors. *J Am Chem Soc.* 2008;130:17697–17709.
- [53] Fukui KFH. *Frontier orbitals and reaction paths.* Singapore: World Scientific Publishing; 1997.
- [54] Cnubben N. Quantitative structure activity relationships for the biotransformation and toxicity of

- halogenated benzene-derivatives: implications for enzyme catalysis and reaction mechanisms. Wageningen: University of Wageningen; 1996.
- [55] Fleming I. Radical reactions. In: Fleming J, editor. Frontier orbitals and organic chemical reactions. New York: John Wiley and Sons; 1989. p. 182–186.
- [56] Klopman G. Chemical-reactivity and the concept of charge-controlled and frontier-controlled reactions. *J Am Chem Sci*. 1968;90:223–234.
- [57] Tauber J, Imbri D, Opatz T. Radical addition to iminium ions and cationic heterocycles. *Molecules*. 2014; 19:16190–16222.
- [58] Braterman PS, Song JI. Spectroelectrochemistry of aromatic ligands and their derivatives.1. reduction products of 4,4'-bipyridine, 2,2'-bipyridine, 2,2'-bipyrimidine, and some quaternized derivatives. *J Org Chem*. 1991;56:4678–4682.
- [59] Jain A, Ramanathan V, Sankararamkrishnan R. Lone pair... pi interactions between water oxygens and aromatic residues: quantum chemical studies based on high-resolution protein structures and model compounds. *Prot Sci*. 2009;18:NA-605.
- [60] Egli M. On stacking. In: Compa P, editor. Structure and function. London (UK): Springer; 2010. p. 188.
- [61] Matsumoto K, Hayashi N. Heterocyclic supramolecules II. Berlin: Springer-Verlag; 2009. p. 27.
- [62] Scheiner S, Kar T, Pattanayak J. Comparison of various types of hydrogen bonds involving aromatic amino acids. *J Am Chem Soc*. 2002;124:13257–13264.
- [63] Ahlberg E, Hammerich O, Parker VD. Electron-transfer reactions accompanied by large structural-changes.1. lucigenin-10,10'-dimethyl-9,9'-biacridylidene redox system. *J Am Chem Soc*. 1981;103:844–849.
- [64] Huang J, Mara MW, Stickrath AB, Kokhan O, Harpham MR, Haldrup K, et al. A strong steric hindrance effect on ground state, excited state, and charge separated state properties of a Cu-I-diimine complex captured by X-ray transient absorption spectroscopy. *Dalton Trans*. 2014;43:17615–17623.
- [65] DiLabio GA, Johnson ER. Lone pair-pi and pi-pi interactions play an important role in proton-coupled electron transfer reactions. *J Am Chem Soc*. 2007;129: 6199–6203.
- [66] Yoshida K, Cheynier V, Quideau S. Recent advances in polyphenol research. New York: Wiley Blackwell; 2017. p. 15–17.
- [67] Zhang H-Y, Sun Y-M, Zhang G-Q, Chen D-Z. Why static molecular parameters cannot characterize the free radical scavenging activity of phenolic antioxidants. *Quant Struct-Act Relat*. 2000;19:375–379.
- [68] Jeremic S. Importance of hydrogen bonding and aromaticity indices in QSAR modeling of the antioxidative capacity of selected (poly)phenolic antioxidants. *J Mol Graph Model*. 2017;72:240–245.
- [69] Fuller T. Proton exchange membrane fuel cells 8. Vol. 16, ECS Transactions. Proceedings of a meeting held; PRiME 2008; 2008 Oct 12–17; Honolulu, Hawaii, USA; 2008.
- [70] Nakarada D, Petkovic M. Mechanistic insights on how hydroquinone disarms OH and OOH radicals. *Int J Quantum Chem*. 2018;118:e25496.
- [71] Mishra R, Mukhopadhyay S, Banerjee R. Reduction mechanism of a coordinated superoxide by thiols in acidic media. *Dalton Trans*. 2010;39:2692–2696.
- [72] Cardey B, Foley S, Enescu M. Mechanism of thiol oxidation by the superoxide radical. *J Phys Chem A*. 2007;111:13046–13052.
- [73] De Matteis F, Lord GA, Kee Lim C, Pons N. Bilirubin degradation by uncoupled cytochrome P450. Comparison with a chemical oxidation system and characterization of the products by high-performance liquid chromatography/electrospray ionization mass spectrometry. *Rapid Commun Mass Spectrom*. 2006; 20:1209–1217.
- [74] Shukla AK, Singh KN. Phase transfer reaction of potassium superoxide with benzylic methyl and methylene compounds in aprotic medium. *Ind J Chem Technol*. 2004;11:848–852.
- [75] Zhu QY, Zhang XM, Fry AJ. Bond dissociation energies of antioxidants. *Polym Degrad Stabil*. 1997;57:43–50.
- [76] Steigerwald ML, Goddard WA, Evans DA. Theoretical studies of the oxy anionic substituent effect. *J Am Chem Soc*. 1979;101:1994–1997.
- [77] Frimer AA, Farkash-Solomon T, Aljadeff G. Mechanism of the superoxide anion radical ( $O_2^{\bullet -}$ ) mediated oxidation of diarylmethanes. *J Org Chem*. 1986;51: 2093–2098.
- [78] Dhaouadi Z, Nsangou M, Garrab N, Anouar EH, Marakchi K, Lahmar S. DFT study of the reaction of quercetin with  $O_2^{\bullet -}$  and OH radicals. *J Mol Struct Theochem*. 2009;904:35–42.
- [79] Ali HM, Ali IH. QSAR and mechanisms of radical scavenging activity of phenolic and anilinic compounds using structural, electronic, kinetic, and thermodynamic parameters. *Med Chem Res*. 2015;24: 987–998.
- [80] Song Y, Buettner GR. Thermodynamic and kinetic considerations for the reaction of semiquinone radicals to form superoxide and hydrogen peroxide. *Free Radic Biol Med*. 2010;49:919–962.
- [81] Taubert D, Breitenbach T, Lazar A, Censarek P, Harlfinger S, Berkels R, et al. Reaction rate constants of superoxide scavenging by plant antioxidants. *Free Radic Biol Med*. 2003;35:1599–1607.
- [82] Nadezhdin AD, Dunford HB. Oxidation of ascorbic-acid and hydroquinone by perhydroxyl radicals - flash-photolysis study. *Can J Chem*. 1979;57:3017–3022.
- [83] Nauser T, Casi G, Koppenol WH, Schöneich C. Reversible intramolecular hydrogen transfer between cysteine thiol radicals and glycine and alanine in model peptides: absolute rate constants derived from pulse radiolysis and laser flash photolysis. *J Phys Chem B*. 2008;112:15034–15044.
- [84] Mayer JM, Hrovat DA, Thomas JL, Borden WT. Proton-coupled electron transfer versus hydrogen atom transfer in benzyl/toluene, methoxyl/methanol, and phenoxy/phenol self-exchange reactions. *J Am Chem Soc*. 2002;124:11142–11147.
- [85] Hammes-Schiffer S. Proton-coupled electron transfer: classification scheme and guide to theoretical methods. *Energy Environ Sci*. 2012;5:7696–7703.
- [86] Quintero-Saumeth J, Rincón DA, Doerr M, Daza MC. Concerted double proton-transfer electron-transfer

- between catechol and superoxide radical anion. *Phys Chem Chem Phys*. 2017;19:26179–26190.
- [87] Wirz J. Kinetic studies of keto-enol and other tautomeric equilibria by flash photolysis. *Adv Phys Org Chem*. 2010;44:325–356.
- [88] Srinivasarao L, Venkatachalapathi V, Venkataramiah K. Halogen substituted amides.1. CNDO calculation of N-methylcarbonyl chloride and N-chloroacetamide. *Proc Indian Acad Sci Sect A*. 1975;81:256–261.
- [89] Tejero I, González-García N, González-Lafont À, Lluç JM. Tunneling in green tea: Understanding the antioxidant activity of catechol-containing compounds. A variational transition-state theory study. *J Am Chem Soc*. 2007;129:5846–5854.
- [90] Wigner E. Crossing of potential thresholds in chemical reactions. *Z Phys Chem*. 1932;81:203–216.
- [91] Gilroy JB, McKinnon SDJ, Koivisto BD, Hicks RG. Electrochemical studies of verdazyl radicals. *Org Lett*. 2007;9:4837–4840.
- [92] Samuni A, Krishna CM, Mitchell JB, Collins CR, Russo A. Superoxide reaction with nitroxides. *Free Radic Res Commun*. 1990;9:241–249.
- [93] Amos RIJ, Chan B, Easton CJ, Radom L. Hydrogen-atom abstraction from a model amino acid: dependence on the attacking radical. *J Phys Chem B*. 2015; 119:783–788.
- [94] Lespade P. On the importance of water molecules in the theoretical study of polyphenols reactivity toward superoxide anion. *J Theor Chem*. 2014;2014:1.
- [95] Su YO, Kuwana T, Chen SM. Electrocatalysis of oxygen reduction by water-soluble iron porphyrins – thermodynamic and kinetic advantage studies. *Electroanal Chem*. 1990;288:177–195.
- [96] Amic D, Davidovic-Amic D, Beslo D, Rastija V, Lucic B, Trinajstić N. SAR and QSAR of the antioxidant activity of flavonoids. *CMC*. 2007;14:827–845.